

An Experimental and Theoretical Study of Hollow Cathode Plume Mode Oscillations

IEPC-2017-298

*Presented at the 35th International Electric Propulsion Conference
Georgia Institute of Technology – Atlanta, Georgia – USA
October 8–12, 2017*

Marcel P. Georjin,^{*} Benjamin A. Jorns,[†] and Alec D. Gallimore[‡]
University of Michigan, Ann Arbor, Michigan, 48109, USA

The oscillations associated with the onset of “plume mode” in a hollow cathode are analytically and experimentally characterized. An analytical model for the plume mode oscillation that is driven by the onset of ion acoustic turbulence in the hollow cathode plume is derived from first principles. This model predicts that the plume mode oscillation should have an acoustic dispersion relation. The dispersion relation of the cathode plume mode was measured experimentally using a high-speed camera. The measured phase velocity is in good agreement with the prediction of the analytical model. No stability criterion was found through this model. The lack of stability criteria is discussed.

Nomenclature

\dot{m}	=	Mass flow rate
ϵ	=	Dispersion
ϵ_0	=	Permittivity of free space
ν_{an}	=	Anomalous collision frequency
ν_{in}	=	Ion neutral collision frequency
ω	=	Plume mode oscillation frequency
ω_0	=	Mean frequency of ion acoustic turbulence
\tilde{I}	=	Light intensity fluctuation
\tilde{n}	=	Density fluctuation
c_s	=	Ion sound speed
E	=	Electric field
I	=	Discharge current
k	=	Plume mode oscillation wave vector
M_e	=	Electron Mach number
n_e	=	Electron number density
n_i	=	Ion number density
T_e	=	Electron temperature
T_i	=	Ion temperature
u_e	=	Electron drift velocity
u_i	=	Ion drift velocity
v_e	=	Electron thermal speed
v_{ph}	=	Phase velocity
W_T	=	Ion acoustic wave energy density

^{*}Ph.D. Candidate, Applied Physics, marcel.georjin@umich.edu

[†]Assistant Professor, Aerospace Engineering, benjamin.jorns@umich.edu

[‡]Robert J. Vlasic Dean of Engineering, Aerospace Engineering, alec.gallimore@umich.edu

I. Introduction

HOLLOW cathodes are quasi-neutral plasma devices that are typically used as electron current sources. Cathodes use low work-function materials such as LaB₆ or BaO as thermionic emitters to supply electrons to the plasma at low voltage. They are used in electric propulsion devices, like Hall thrusters and gridded ion thrusters, as discharge current sources and ion beam neutralizers. These cathodes are known to have two distinct discharge modes, the so-called spot and plume modes. Figure 1a shows a cathode operating in spot mode. This type of discharge is relatively dim except at the orifice of the cathode and the discharge current (or voltage) oscillations are small. Figure 1b shows a cathode operating in plume mode. Not only is there a visible change in the discharge, but the properties of the plasma change. The discharge voltage typically rises by several volts and the plasma current (or voltage) oscillations are almost on the order of the steady state current (or voltage). In addition to the onset of these plasma oscillations, the plume mode is highly erosive and can destroy the keeper electrode. The keeper erosion as a result of operating in the plume mode can limit the lifetime of the cathode and the overall electric propulsion system.^{1,2}

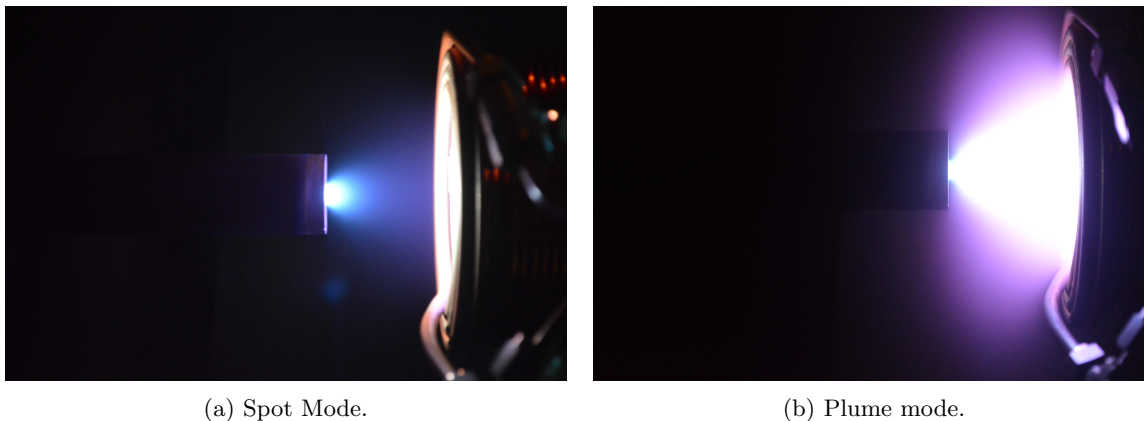


Figure 1: A comparison of the cathode modes. The hollow cathode is on the left and the anode is on the right.

Although hollow cathodes have been used in space for decades, there is still no complete physical description of why the plume mode onsets. Previous experimental³⁻⁶ at characterizing the plume mode transition have determined an empirical onset criterion,

$$\frac{I}{\dot{m}} > \alpha, \quad (1)$$

where I is the discharge current in [A], \dot{m} is the mass flow rate through the cathode in [sccm], and $\alpha \sim \mathcal{O}(1 - 10)$ is a constant. Physically, this instability criterion has been interpreted as the onset requirement of ionization-like predator prey modes.^{7,8} In this model, the electrons are predators and the neutrals are the prey. If the current is increased sufficiently for a fixed mass flow rate, then the electron density and ionization fraction rise. Above some threshold, electron will ionize too many neutrals and the ionization rate will begin to decrease because of the reduced neutral density. As a result, the electron density will subsequently decrease. This oscillatory behavior between the electrons and ions is called the predator-prey model. This physical interpretation has yet to be confirmed numerically, analytically, or experimentally and is not always correct.

These empirical laws have guided the design of hollow cathodes for several decades and have resulted in many for Earth orbiting electric spacecraft. However, for deep-space missions with life requirements exceed 50,000 hours it is important to have a physical description of this erosive transition such that the following questions can be answered. First, will the cathode plume mode onset over the course of the mission and dramatically reduce thruster lifetime? Typically, to answer this questions it is common to conduct life tests of stand-alone hollow cathodes to ensure the device can meet the mission requirements. However, life testing to the mission requirements is prohibitively time consuming and expensive for deep space missions. Furthermore, stand-alone hollow cathode life tests do not necessarily replicate the erosion characteristics during thruster operation. This means that to get an accurate estimate of the cathode lifetime, a full life

test of the thruster is required.¹ Second, can cathode behavior on orbit be predicted? Vacuum facilities are also known to affect the performance of plasma propulsion devices, meaning performance on orbit cannot always be predicted.^{9–12} In particular, changes in facility pressure can dictate the transition to plume mode. To overcome these obstacles, there is an apparent need to understand the fundamental physics of hollow cathodes such that high-fidelity numerical models can be developed for flight qualification and to predict on-orbit behavior. In this work, we present a first attempt at the development of an analytical description of the propagation characteristics of the cathode plume mode oscillation and experimental evidence to support this physical picture.

This paper is organized as follows. First, an overview of relevant hollow cathode physics is provided. Next, we present the development of an analytical model that describes the propagating characteristics of the plume mode wave. Lastly, an experimental measurement of the dispersion relation is used to confirm the analytically derived dispersion relation.

II. Overview of Hollow Cathode Physical Processes

Before we develop our theory for the plume mode we will first provide some background on the relevant hollow cathode physics. Until recently, hollow cathode fluid models were unable to self-consistently model the temperature and potential profiles in the cathode plume.¹³ To match experimental data, the so called “anomalous collision frequency,” ν_{an} , for electrons was included in cathode plume models. More recently, through first principles modeling and experimental measurements, the “anomalous collision frequency” was shown to be a result of an interaction between electrons and ion acoustic turbulent waves.^{14,15} Ion acoustic turbulence (IAT) is an electrostatic plasma instability that grows at the expense of the strong electron drift that is characteristic of the hollow cathode plume. Modern hollow cathode models self-consistently describe the electron temperature and plasma potential through this wave interaction.^{16–18} In a fluid description, these waves introduce an effective drag force on the electrons that leads to frictional heating on ions and electrons. While including this anomalous drag force allows fluid models to more accurately predict the steady state plasma parameters, most numerical models still do not properly resolve the fluctuations in those parameters.

Jorns et.al.¹⁹, Lopez-Ortega et.al.¹⁸, and Sary et. al.^{16,17} have all developed a numerical fluid model that not only includes self-consistent heating. The transport of the IAT energy density can be modeled like a fluid with a wave equation.^{14,19,20}

$$\frac{\partial W_T}{\partial t} + \nabla \cdot ((c_s \hat{u}_i + \vec{u}_i) W_T) = \omega_0 W_T \left(\frac{|u_e - u_i| - c_s}{v_e} - \left(\frac{T_e}{T_i} \right)^{3/2} e^{-\frac{T_e}{2T_i}} - \frac{\nu_{in}}{\omega_0} \right) \quad (2)$$

where W_T is the turbulent wave energy density, u_s are the species drift velocities, v_e is the electron thermal speed, c_s is the ion sound speed, ω_0 is the average frequency of the IAT spectrum, and ν_{in} is the ion neutral collision frequency. The anomalous collision frequency is related to the wave energy by $\nu_{an} \propto \frac{W_T}{nT_e}$. When IAT transport was included in their model, Sary et. al. observed large, coherent amplitude plasma potential and density waves, which agrees with the experimental description of Goebel et. al.⁸ This plasma oscillation is illustrated in Fig. 2, where the red regions are those of higher plasma density. Through this numerical model Sary et. al. have proposed the following mechanism for the instability. Assuming the electron Mach number is sufficiently high to onset IAT, then the wave energy can grow and lead to electron heating. The growth of the IAT quenches itself through electron Landau damping and this region of high plasma density propagates out of the cathode at the IAT phase velocity,

$$v_{ph} = u_i + c_s. \quad (3)$$

With this interpretation, we would expect the growth and saturation process to occur at a fixed frequency, the rate at which wave energy saturates and decays. Since the disturbance propagates at the IAT phase velocity, the phase velocity of the plume mode oscillation is fixed. Combined, these two properties lead to a single wavelength.

Although experiment and simulation are beginning to develop a better understanding of the plume mode, there still remain several gaps in our understanding of this wave. There are still no measurements of the dispersion relation of the wave. There is still no theoretical expression for the dispersion relation or an instability criterion of the wave. In the following sections, we experimentally measure the dispersion relation

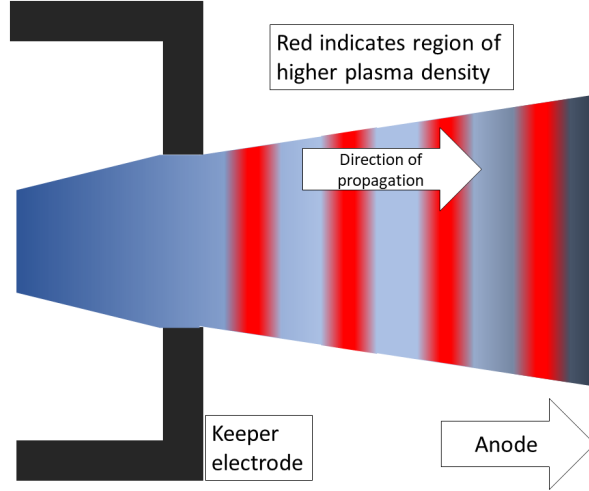


Figure 2: A notional figure of the propagating density oscillation observed by Sary and Goebel. The red regions are those of higher plasma density.

of the cathode plume mode and interpret the results in the context of IAT driven plasma oscillations. Furthermore, we develop a preliminary analytical model to describe the dispersion and instability criteria.

III. Analytical Model

To date, most cathode models are numerical^{13,16–18,21} and few resolve the plume mode oscillation. Moreover, there has been little analytical modelling of the plume mode transition to self-consistently derive an onset criterion for the plume mode oscillation.²² Here, we develop an analytical model for the plume mode oscillation based on the recent numerical results of Sary et. al.^{16,17}, specifically aiming to derive a dispersion relation and an onset criterion.

Numerical hollow cathode models typically solve the fluid equations,^{13,16–18} therefore we will solve the those equations in one dimension including an additional transport equation for the IAT wave energy density. We will assume that the anomalous collision frequency is large compared to the classical collision frequency and the plume mode oscillation frequency. Furthermore, we will assume that the electron drift velocity is much greater than the ion drift velocity. Below is the set of fluid equations on which we will perform a linear perturbation analysis and solve the dispersion.

The equations for electron and ion continuity, respectively, are given by

$$\frac{\partial n_e}{\partial t} + \nabla \cdot (n_e u_e) = 0 \quad (4)$$

$$\frac{\partial n_i}{\partial t} + \nabla \cdot (n_i u_i) = 0, \quad (5)$$

where n_e is the electron density, n_i is the ion density, u_e is the electron drift velocity, and u_i is the ion drift velocity. In Eqns. 4 and 5, contributions from ionization have been ignored. For the momentum equations, we take into consideration the “anomalous” collisional process, which transfers momentum elastically from the electrons to the ions. The electron momentum equation is

$$q \frac{n_e E}{m_e} + \frac{\nabla (n_e T_e)}{m_e} + n_e u_e \nu_{an} (W_T) = 0, \quad (6)$$

where q is the magnitude of the unit charge, m_e is the electron mass, E is the electric field, T_e is the electron temperature, ν_{an} is the anomalous collision frequency, and W_T is the IAT wave energy density. Eqn. 6

ignores the inertial contributions to the electron momentum and is thus written as an Ohm's law. The ion momentum equation is

$$\frac{\partial n_i u_i}{\partial t} + \nabla (n_i u_i^2) = q \frac{n_i E}{m_i} + n_i u_e \nu_{an}(W_T) \frac{m_e}{m_i}, \quad (7)$$

where m_i is the ion mass. Eqn. 7 assumes that the ions are cold and we include the effect of anomalous collisions, which acts as a source of ion momentum, unlike the electrons. Next we have Poisson's equation,

$$\nabla \cdot E = \frac{q}{\epsilon_0} (n_i - n_e). \quad (8)$$

Lastly we include a simplified IAT wave energy density equation,

$$\frac{\partial W_T}{\partial t} = \omega_0 M_e W_T, \quad (9)$$

where $M_e = \frac{u_e}{v_e}$ is the electron Mach number. We have ignored convection of the wave energy and all of the damping terms.

In these expressions, we will perturb the the densities, the velocities, the electric field and the wave energy density. Performing the linear perturbation analysis, such that, for example,

$$n = n_0 + n_1 e^{i(kx - \omega t)}, \quad (10)$$

and using the simplifying assumptions listed above, we solve for the dispersion by substituting the density fluctuations into Poisson's equation to find

$$\epsilon = \frac{1}{(\omega - k u_{i0})^2 - i k v_e \frac{\nu_{an}}{2} M_e \frac{m_e}{m_i}} + \frac{1}{-(k c_s)^2 + i k v_e \frac{\nu_{an}}{2} M_e \frac{m_e}{m_i}} = 0. \quad (11)$$

Rearranging this expression and solving for the real part of the frequency we find that

$$\omega_r = k (u_{i0} + c_s). \quad (12)$$

We find that the phase velocity, ω/k , is at the ion acoustic wave speed. This result matches our expectation for an IAT driven plume mode oscillation, as Sary et. al. showed in their numerical simulations. Next we solve for the imaginary component of the frequency, which should provide a stability criterion; however, we find that

$$\omega_i = 0. \quad (13)$$

In this formulation, we find that there is no growth or stability criterion for this wave. We return to a discussion of the lack of a stability criterion in Sec.VI. Nevertheless, this model predicts a propagating wave at the speed we expect based on the physical interpretation of the plume mode provided by Sary et. al.

IV. Experimental Setup

An experiment was designed to measure the dispersion of the plume mode plasma oscillation using a high-speed camera. The experiment was conducted in the Cathode Test Facility (CTF) at the Plasmadynamics and Electric Propulsion Laboratory (PEPL). The facility has a pumping speed of 1500 L-Xe/s and achieves a base pressure of 7×10^{-7} Torr. During the experiment, the pressure in the facility varied between 5×10^{-5} Torr-Xe and 5×10^{-4} Torr-Xe. The LaB₆ cathode used in this experiment was nominally designed to operate at 20 A of discharge current and has a 2.54 in. diameter keeper and a 3 mm orifice. The hollow cathode was operated between 10 and 25 A of discharge current and between 5 and 15 sccm of Xe to examine the onset of the plume mode. The anode was cylindrical and made of tungsten and placed at a distance of 40 mm from the cathode to provide optical access.

Figure 3 is a notional diagram of the experimental setup. A Fastcam SA-5 high-speed CCD camera was used to image the discharge at 300 kfps through a viewport in the CTF. The pixel intensity can be related

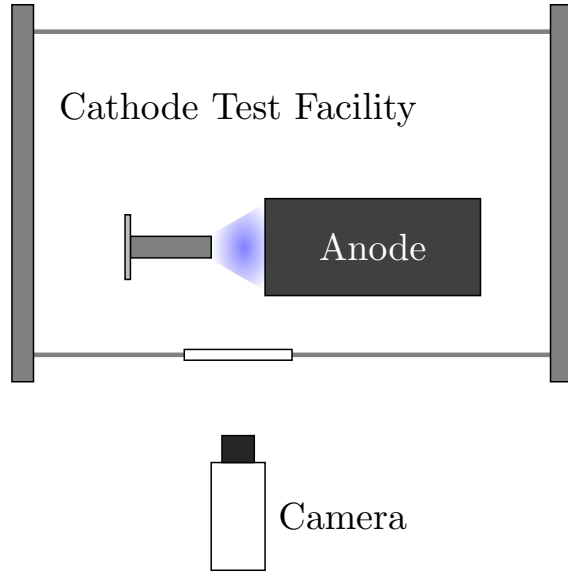


Figure 3: Aerial view of the experimental setup. The cathode and anode are 40 mm apart. The high-speed camera images the discharge from the side.

to density by²³

$$I = n_n n \sigma_0 \sqrt{T_e} \left(1 + \frac{T_e}{\epsilon} \right) \Rightarrow \quad (14)$$

$$\frac{\tilde{I}}{I_0} = \frac{\tilde{n}}{n_0}, \quad (15)$$

where \tilde{I}/I_0 is the relative fluctuation in the light emitted by the plasma, n_n is the neutral density and σ_0 is the average optical emission cross section, and ϵ is the optical emission cutoff energy.^{23,24} This expression can be used when the relative fluctuations of the electron temperature and neutral density are small compared to the relative fluctuation of the plasma density. A similar optical technique has been used to measure incoherent plasma oscillations in hollow cathodes.²³ This non-invasive diagnostic will be used to estimate the dispersion relation of the plume mode.

To estimate the dispersion relation for the plume mode, we will employ the statistical technique employed by Beall.²⁵ This technique has been used extensively to measure waves in hollow cathodes^{14,23} Two pixels sample the wave and the phase between the signals is computed at each frequency in the power spectrum. Based on the distance between the pixels, the wave vector is estimated, resulting in $\omega(k)$. After binning and averaging, the dispersion, $D(\omega, k)$, is estimated. The output of this analysis is a two dimensional color plot where the axes are the frequency and wave vector and the color is the average fluctuation amplitude. This technique was applied to density fluctuations from high-speed imaging.²³

V. Results

We present measurements of a cathode operating in plume mode using a high-speed camera. The intensity fluctuations of the pixels are analyzed using the Beall dispersion technique and the results are curve fit to find the phase velocity.

A. Raw High-speed Images

Still images of the high-speed camera are first examined qualitatively. In these stills, the cathode orifice is on the left of the image and the anode is on the right. Figure 4 shows a time sequence of high-speed video captured at 700 kfps while the cathode is operating at 20 A and 10 sccm. A bright region is formed in the plume near the cathode and propagates downstream to the anode. The bright region is formed periodically at

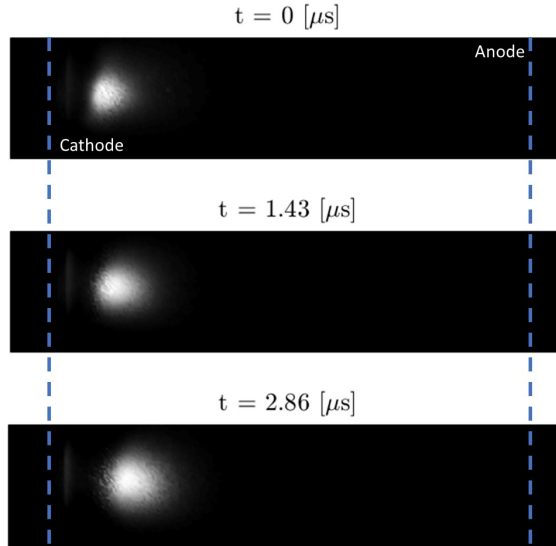


Figure 4: Stills from the high-speed camera captured at 700 kfps. They show the generation of light intensity downstream of the cathode and its propagation. The cathode is on the left and the anode is on the right.

about 50 kHz and consistently in the same location. Qualitatively, these images agree with the interpretation of Sary et. al. A large coherent structure forms near the cathode and propagates towards the anode.

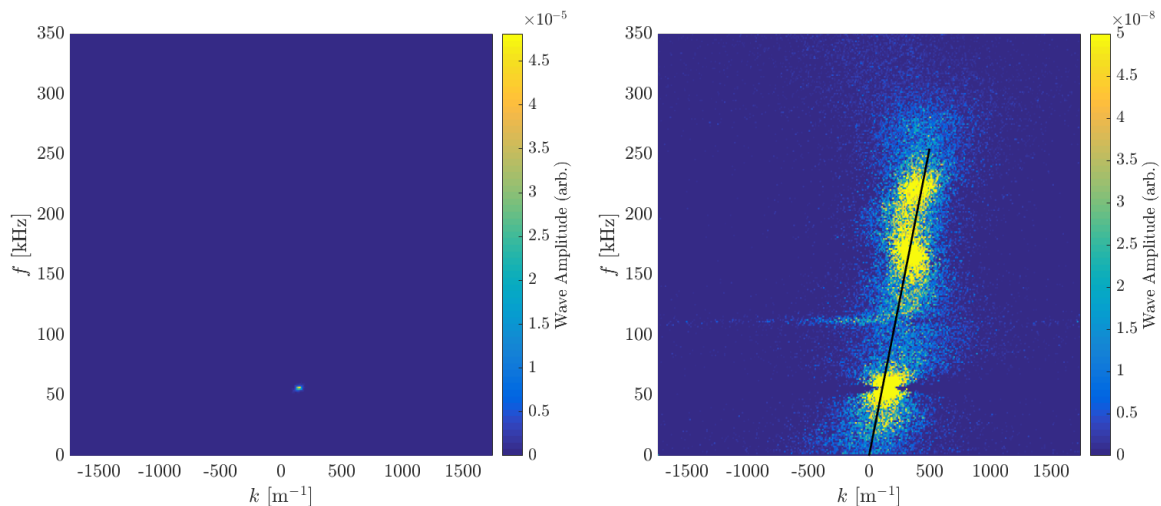
B. Dispersion Relation

To better compare with an IAT driven model of the plume mode, we need to quantify the dispersion relation and phase velocity. Using the Beall technique,²⁵ we have estimated the dispersion relation of the cathode plume mode oscillation. Figure 5 shows the estimated dispersion relation for the cathode operating in the plume mode at 20 A and 5 sccm. The measurement uses two pixels that capture light at 10 mm downstream of the keeper. Figure 5a shows the raw dispersion. A distinct single frequency and wavelength are the dominant mode at $f = 50$ [kHz] and $k = 98$ [1/m]. Figure 5b saturates the color axis to show detail in the dispersion relation. In this figure, the frequency of oscillation is clearly proportional to the wave vector, $\omega \propto k$. The curve fit finds a phase velocity for the plume mode of 3.2 km/s. Based on estimates from the literature, we know that the ion drift velocity is about 2 km/s and the ion sound speed is about 1.5 km/s. Our analytical model then predicts a phase velocity of 3.5 km/s, which is in good agreement with the measured phase velocity of the mode.

The Sary model of the plume mode predicts a single unstable frequency and wavelength with a phase velocity at the ion acoustic wave speed. These are in agreement with the properties measured by the high-speed camera. We also note that the wavelength, $\lambda = 64$ mm is close to the separation of the anode and the cathode (40 mm). This similarity suggests that the wavelength of the oscillation may be tied to the geometry of the experimental setup.

VI. Discussion

Now we will discuss the implications of our results in light of our analytical model and the numerical simulations of Sary et. al. Our analytical theory for the plume mode oscillation predicted an acoustic dispersion relation with a phase velocity of the sum of the ion drift and sound speeds. The dispersion relation measured by the high-speed camera was in good agreement with the analytical model. However, this result alone does not prove that the instability is driven by acoustic turbulence. Predator-prey type ionization instabilities would also likely propagate at the approximately velocity. As ions are generated by ionization, they propagate towards the anode at the ion drift speed. When Sary et. al. removed the wave energy equation from their model, they did not find oscillations. These measurements, combined with the numerical results from Sary et. al. and our analytical model suggest that a simple ionization wave description



(a) Unsaturated dispersion shows a single dominant frequency and wavelength. (b) Saturated dispersion shows and acoustic relationship. The curve fit shows a phase velocity of 3.2 km/s.

Figure 5: The estimated dispersion from the high-speed camera. The cathode was operating at 20 A of discharge current and 5 sccm of Xe at 10 mm from the keeper surface.

of the plume mode may be an oversimplification and that IAT may play a role in the onset of the plume mode.

Our relatively simple analytical model, was unable to recover an instability criterion. In our model, we include a mechanism for growth of the wave energy density. Based on the physical interpretation of Sary et. al., we would expect to perhaps found that the mode should at least be unconditionally unstable. Since we have no stability criteria, this suggests the wave energy density is poorly coupled to the standard set of fluid equations. In our model, we have made a simplifying assumption that electron temperature fluctuations were small. However, the simulation work by Sary et.al. shows that the electron temperature may be fluctuating by a few electron volts. Including an electron energy equation and perturbing the electron temperature may lead to instability. The analytical model will be revisited including this temperature fluctuation.

VII. Conclusion

The plasma oscillation that generates the cathode plume mode has been treated analytically and interpreted in the light of recent numerical simulations that show the importance of ion acoustic turbulence in the transient behavior of the cathode. We have shown that the dispersion relation for the plume mode oscillation should be acoustic with a phase velocity at the ion acoustic wave speed. This relationship has been verified through experimental measurements of the dispersion relation using a high-speed camera imaging technique. The analytical model, however, fails to identify a stability criterion and a clear source of energy for the onset of the instability. This may be a result of poor coupling between the wave energy equation and the standard fluid equations. Including temperature fluctuations in the analytical model may eventually provide an instability criterion.

Overall, our experimental measurements have provided new insight into the propagating characteristics of the plume mode oscillations. Further theoretical investigation should eventually provide an instability criterion and a physical interpretation for the energy source of the plume mode instability. Lastly, these results could then be used to improve the fidelity of numerical models for life-time qualification for deep-space missions.

Acknowledgments

This work was funded by the NASA Space Technology Research Fellowship under grant NNX15AQ37H.

References

- ¹ Sengupta, A., Brophy, J., Anderson, J., Garner, C., Banks, B., and Groh, K., “An Overview of the Results from the 30,000 Hr Life Test of Deep Space 1 Flight Spare Ion Engine,” *40th AIAA/ASME/SAE/ASEE Joint Propulsion Conference and Exhibit*, No. 3608, American Institute of Aeronautics and Astronautics, July 2004.
- ² Mikellides, I. G., Katz, I., Goebel, D. M., Jameson, K. K., and Polk, J. E., “Wear mechanisms in electron sources for ion propulsion, II: Discharge hollow cathode,” *Journal of Propulsion and Power*, Vol. 24, No. 4, 2008, pp. 866–879.
- ³ Csiky, G. A., “Measurements of some properties of a discharge from a hollow cathode,” *NASA Technical Note*, 1969.
- ⁴ Philip, C., “A Study of Hollow Cathode Discharge Characteristics,” *AIAA Journal*, Vol. 9, No. 11, Nov. 1971, pp. 2191–2196.
- ⁵ Domonkos, M. T., Gallimore, A. D., Williams Jr, G. J., and Patterson, M. J., “Low-current hollow cathode evaluation,” *Joint Propulsion Conference*, No. 2575, American Institute of Aeronautics and Astronautics, Los Angeles, CA, 1999, p. 48109.
- ⁶ Williams, G.J., J., Smith, T., Domonkos, M., Gallimore, A., and Drake, R., “Laser-induced fluorescence characterization of ions emitted from hollow cathodes,” *IEEE Transactions on Plasma Science*, Vol. 28, No. 5, Oct. 2000, pp. 1664–1675.
- ⁷ Fife, J., Martinez-Sanchez, M., Szabo, J., Fife, J., Martinez-Sanchez, M., and Szabo, J., “A numerical study of low-frequency discharge oscillations in Hall thrusters,” American Institute of Aeronautics and Astronautics, July 1997.
- ⁸ Goebel, D. M., Watkins, R. M., and Jameson, K. K., “LaB6 hollow cathodes for ion and hall thrusters,” *Journal of propulsion and power*, Vol. 23, No. 3, 2007, pp. 552–558.
- ⁹ Randolph, T., Kim, V., Kaufman, H., Kozubsky, K., Zhurin, V. V., and Day, M., “Facility effects on stationary plasma thruster testing,” *23rd International Electric Propulsion Conference*, No. 844, 1993, pp. 13–16.
- ¹⁰ Walker, M. L. R., Victor, A. L., Hofer, R. R., and Gallimore, A. D., “Effect of Backpressure on Ion Current Density Measurements in Hall Thruster Plumes,” *Journal of Propulsion and Power*, Vol. 21, No. 3, 2005, pp. 408–415.
- ¹¹ Reid, B. M., “Empirically-Derived Corrections for Facility Effects in Performance and Plume Measurements of Hall Thrusters,” *23rd International Electric Propulsion Conference*, No. 326, Kobe, Japan, July 2015.
- ¹² Hofer, R. R., Johnson, L. K., Goebel, D. M., and Wirz, R. E., “Effects of internally mounted cathodes on Hall thruster plume properties,” *Plasma Science, IEEE Transactions on*, Vol. 36, No. 5, 2008, pp. 2004–2014.
- ¹³ Mikellides, I. G., Katz, I., Goebel, D. M., and Jameson, K. K., “Evidence of nonclassical plasma transport in hollow cathodes for electric propulsion,” *Journal of Applied Physics*, Vol. 101, No. 6, March 2007, pp. 063301.
- ¹⁴ Jorns, B. A., Dodson, C., Goebel, D. M., and Wirz, R., “Propagation of ion acoustic wave energy in the plume of a high-current LaB6 hollow cathode,” *Physical Review E*, Vol. 96, No. 2, Aug. 2017, pp. 023208.
- ¹⁵ Yanes, N., Jorns, B., Friss, A., Polk, J. E., Guerrero, P., and Austin, J. M., “Ion Acoustic Turbulence and Ion Energy Measurements in the Plume of the HERMeS Thruster Hollow Cathode,” *23rd International Electric Propulsion Conference*, No. 5028, American Institute of Aeronautics and Astronautics, Kobe, Japan, July 2016.
- ¹⁶ Sary, G., Garrigues, L., and Boeuf, J.-P., “Hollow cathode modeling: I. A coupled plasma thermal two-dimensional model,” *Plasma Sources Science and Technology*, Vol. 26, No. 5, 2017, pp. 055007.

- ¹⁷ Sary, G., Garrigues, L., and Boeuf, J.-P., “Hollow cathode modeling: II. Physical analysis and parametric study,” *Plasma Sources Science and Technology*, Vol. 26, No. 5, 2017, pp. 055008.
- ¹⁸ Lopez Ortega, A., Mikellides, I. G., and Jorns, B., “First-principles modeling of the IAT-driven anomalous resistivity in hollow cathode discharges II: Numerical simulations and comparison with measurements,” American Institute of Aeronautics and Astronautics, July 2016.
- ¹⁹ Jorns, B., Lopez Ortega, A., and Mikellides, I. G., “First-principles Modelling of the IAT-driven Anomalous Resistivity in Hollow Cathode Discharges I: Theory,” American Institute of Aeronautics and Astronautics, July 2016.
- ²⁰ Stix, T. H., *The Theory of Plasma Waves*, 1962.
- ²¹ Katz, I., Anderson, J. R., Polk, J. E., and Brophy, J. R., “One-dimensional hollow cathode model,” *Journal of Propulsion and Power*, Vol. 19, No. 4, 2003, pp. 595–600.
- ²² Mandell, M. and Katz, I., “Theory of hollow operation in spot and plume modes,” American Institute of Aeronautics and Astronautics, June 1994.
- ²³ Georgin, M. P., Byrne, M., Jorns, B. A., and Gallimore, A., “Passive High-speed Imaging of Ion Acoustic Turbulence in a Hollow Cathode,” *53rd AIAA/SAE/ASEE Joint Propulsion Conference*, No. 4973, American Institute of Aeronautics and Astronautics, 2017, DOI: 10.2514/6.2017-4973.
- ²⁴ Kanik, I., Johnson, P. V., and James, G. K., “Electron-impact-induced emission and excitation cross sections of xenon at low energies,” *Journal of Physics B: Atomic, Molecular and Optical Physics*, Vol. 34, No. 9, 2001, pp. 1685.
- ²⁵ Beall, J. M., Kim, Y. C., and Powers, E. J., “Estimation of wavenumber and frequency spectra using fixed probe pairs,” *Journal of Applied Physics*, Vol. 53, No. 6, June 1982, pp. 3933–3940.